ISSN: 2594-3421 (Print), 2773-8191 (Online)

BMC JOURNAL OF SCIENTIFIC RESEARCH

A Multidisciplinary Peer Reviewed Research Journal

Volume 6 December 2023

Published by:
Research Management Cell
Birendra Multiple Campus
Bharatpur, Chitwan, Nepal

Publisher:
Research Management Cell
Birendra Multiple Campus, Bharatpur, Chitwan, Nepal
E-mail: rmcbirendra@gmail.com

ISSN: 2594-3421 (Print), 2773-8191 (Online)

Printed in **Siddhababa Offset Press**, Bharatpur, Chitwan, Nepal, Contact: 9855050040

Price : 200/-

Contents

BMC JOURNAL OF SCIENTIFIC RESEARCH
A Multidisciplinary Peer Reviewed Research Journal
ISSN: 2594-3421 (Print), 2773-8191 (Online)

Theoretical Investigation of the Thermodynamic Properties of Lead-free Ternary Alloys Sn-Sb-Bi and their Subsystems

Sanjay Kumar Sah[1,2*], Indu Shekhar Jha[3], Ishwar Koirala[1]

[1]Central Department of Physics, Tribhuvan University, Kirtipur, Kathmandu, Nepal
[2]Department of Physics, Birendra Multiple Campus, Tribhuvan University, Bharatpur, Nepal
[3]Department of Physics, M.M.A.M. Campus, Tribhuvan University, Biratnagar, Nepal
[*]Corresponding author: sanjay.sah@bimc.tu.edu.np

Received: May 21, 2023, Accepted: Nov. 1, 2023

Abstract

The concentration-dependent properties, like the constituents' activities for the binary liquid alloys like Sb-Sn at 905 K, Bi-Sn at 600 K, and Bi-Sb at 1200 K, and the integral Gibbs free energy of mixing, ΔG^{XS}, of the correspondent alloys were computed using the molecular interaction volume model (MIVM). Further, the model has been used to compute the activities of the component Sn in the ternary Sn-Sb-Bi system at 900K at the three cross-sections, i.e., Sb:Bi = 1:3, 1:1, and 3:1. The theoretical data have been analyzed with the corresponding experimental data accessible in the literature. An acceptable concurrence has been obtained, with some inconsistencies. The activities of the ternary alloys along the three cross-sections, i.e., Sb:Bi = 1:3, 1:1, and 3:1, show that the deviations change from positive to negative with increasing Sb content. The results confirm that MIVM is a good model for estimating the thermodynamic properties of binary and ternary systems.

Keywords: *Binary liquid alloys, excess Gibbs free energy, lead-free solder alloys, molecular interaction volume model, ternary liquid alloys.*

1. Introduction

Lead-based solder has been widely used in electronic and electrical applications for decades due to its excellent soldering properties, low melting point, and cost-effectiveness. However, the toxicity of lead and its harmful environmental effects have led to strict regulations, such as the European Union's RoHS (Restriction of Hazardous Substances) directive, which restricts the use of lead in electronic and electrical equipment. (Abtew & Selvaduray, 2000; Hindler et al., 2010; Knott & Mikula, 2002; Liang et al., 2021; Moelans et al., 2003). Therefore, in the present era, the utilization of lead has been prohibited globally (Suganuma, 2001). As a result, the electronics industry has been actively researching and developing lead-free solder alternatives. (Knott & Mikula, 2002). Tin (Sn) has been found to be a suitable substitute for lead (Pb) which lies in the periodic table in the same group. The newly developed alloys should possess comparable melting points and other properties such as fatigue resistance, joint strength, corrosion resistance, low cost, non-toxicity, etc. Consequently, numerous attempts have been undertaken by researchers to substitute lead in solder alloys (Almeida et al., 2013; Odusote et al., 2016).

To replace conventional lead-based solders, various types of lead-free solder alloys have been researched and created. These alloys fall into the following major categories: Tin-based alloys, bismuth-based alloys, and other alloys. Tin is a soft silvery-white metal with a lower melting point (505 K) that adds shine to materials, and tin-based alloys are corrosion-resistant (Sah et al., 2022). One of the main properties of Bi is that when Bi alloys solidify, they expand slightly. For this reason, Bi has also been used in the soldering process. This solder gives good wetting and solder flow. Furthermore, Bi has a lower melting point (544.4 K), and its alloys are mostly used for fire detection and suppressing system safety devices. Antimony, Sb, has a melting point of 903.6 K, and its metallic form is bright, silvery, hard, and brittle. So, it is also applicable to solder alloys.

In this overview, we will address the literature that is currently available on lead-free solder alloys as well as the unique difficulties that come with their adoption in soldering technology. Replacing lead-based solder with lead-free alternatives presents several challenges. Lead-free solder alloys generally have higher melting points compared to traditional lead-based solders. This can lead to thermal stress on electronic components during soldering, potentially causing damage. Researchers and manufacturers have been actively working to address the challenges associated with lead-free soldering. The existing literature on lead-free solder alloys includes studies on: Several binary, ternary, and multicomponent alloy systems, including Sn-Cu, Sn-Ag, Zn-In-Sn, Sn-Au-Cu, Sn-Bi-Cu, Sn-Ag-Cu, In-Bi-Sn, Sn-Ag-Cu-Sb, and Sn-Ag-Cu-Zn, among others, have been effectively utilized as superior substitutes for traditional Sn-Pb alloy (Amore et al., 2008; Lee et al., 2004; Sah, Jha, et al., 2023; Sah, Koirala, et al., 2023; Sah & Koirala, 2023). A model of complex formation was employed to examine the thermodynamic properties of liquid alloys composed of Bi-Sb, Bi-Sn, and Sb-Sn by Adedipe et al. (Adedipe et al., 2019). Asryan et al. conducted investigations on the thermodynamic properties of systems containing Bi and Sn within the temperature range of 673 to 793 K using liquid-electrolyte emf measurements (Asryan, N.A., & Mikula, 2004). The model of a quasi-lattice was employed to investigate the thermodynamic characteristics of liquid alloys composed of Sb-Sn and In-Sn (Anusionwu, 2006). The activities of tin in liquid Sn-Bi, Sn-Sn, and Sn-Sb-Bi alloys were determined by measuring the electromotive force (emf) in a galvanic cell with a fused salt electrolyte in the temperature range of 700 to 1000 K for the entire composition range by Katayama et al. (Katayama et al., 2005). This was an experimental method, and there was a lack of study of the thermodynamic properties of the Bi-Sb sub-binary system in the study of Katayama et al. The activity of all components in Bi-Sb-Sn was predicted by Awe et al. in 2014 in three cross-sections taken from the corner of each metal, with the molar ratios of the other two components being 1:3, 1:1, and 3:1 in the temperature range of 500–1000 K (Awe & Oshakuade, 2014). However, the thermodynamic properties of all its sub-binary systems have not been studied yet. Thus, in this study, the molecular

interaction volume model (MIVM) has been utilized to determine the thermodynamic activities of the constituent elements in Sb-Sn binary liquid alloys at 905 K, Bi-Sn at 600 K, and Bi-Sb at 1200 K. The excess Gibbs free energy of mixing, ΔG^{XS}, for these binary alloys has also been calculated. Furthermore, the model has been applied to ascertain the behavior of Sn in Sn-Sb-Bi ternary liquid alloys at a temperature of 900 K across three different compositions, namely X_{Sb}: X_{Bi} = 1:3, 1:1, and 3:1, by varying the concentration of Sn (X_{Sn}).

2. Theory (Methodology)

MIVM (Molecular Interaction Volume Model) originates from a physical standpoint and explores the migration characteristics of liquid molecules. They don't move randomly like gas molecules, which are continually in motion. They also don't move in the same way as solid molecules, which vibrate in one location while also moving from one area to another in a deliberate, orderly manner. The liquid molecules migrate non-randomly inside the molecular cells, which serve as migration carriers. More information about this can be found in the reference (Tao, 2008). It is a two-parameter model that can predict the thermodynamic characteristics of a multicomponent mixture using only the regular physical quantities of pure liquid metals and the associated binary infinite dilute activity coefficient (Tao et al., 2002). The molar excess Gibbs energy, ΔG^{XS}, of the binary liquid mixture i-j can be written as follows when the molecular pair interaction is taken into account (Tao, 2000):

$$\Delta G^{XS} = RT\left\{x_i \ln\left(\frac{V_{mi}}{x_i V_{mi} + x_j V_{mj} A_{ji}}\right) + x_j \ln\left(\frac{V_{mj}}{x_j V_{mj} + x_i V_{mi} A_{ij}}\right) - \frac{x_i x_j}{2}\left(\frac{Z_i A_{ji} \ln A_{ji}}{x_i + x_j A_{ji}} + \frac{Z_j A_{ij} \ln A_{ij}}{x_j + x_i A_{ij}}\right)\right\} \quad \ldots (1)$$

where Z_i and Z_j are the first coordination numbers, R is the universal gas constant, T is the mixing temperature, x_i and x_j are the component i and j's molar fractions, V_{mi} and V_{mj} are their molar volumes, and A_{ij} and A_{ji} are the pair-potential energy interaction parameters, which are defined, respectively, as (Tao, 2000):

$$A_{ji} = \exp\left(-\frac{\varepsilon_{ji} - \varepsilon_{ii}}{KT}\right) ; A_{ij} = \exp\left(-\frac{\varepsilon_{ij} - \varepsilon_{jj}}{KT}\right) \quad \ldots (2)$$

"ε_{ji}" refers to the potential energy between a central i atom and its first nearby j atom, and K represents the Boltzmann constant.

The liquid alloy's components i and j each have activity coefficients of γ_i and γ_j, which are expressed as follows (Tao, 2000):

$$\ln \gamma_i = \ln\left(\frac{V_{mi}}{x_i V_{mi} + x_j V_{mj} A_{ji}}\right) + x_j\left(\frac{V_{mj} A_{ji}}{x_i V_{mi} + x_j V_{mj} A_{ji}} - \frac{V_{mi} A_{ij}}{x_j V_{mj} + x_i V_{mi} A_{ij}}\right) - \frac{x_j^2}{2}\left[\frac{Z_i A_{ji}^2 \ln A_{ji}}{\left(x_i + x_j A_{ji}\right)^2} + \frac{Z_j A_{ij}^2 \ln A_{ij}}{\left(x_j + x_i A_{ij}\right)^2}\right] \quad \ldots (3)$$

$$\ln \gamma_j = \ln\left(\frac{V_{mj}}{x_j V_{mj} + x_i V_{mi} A_{ij}}\right) - x_i\left(\frac{V_{mj} A_{ji}}{x_i V_{mi} + x_j V_{mj} A_{ji}} - \frac{V_{mi} A_{ij}}{x_j V_{mj} + x_i V_{mi} A_{ij}}\right) - \frac{x_i^2}{2}\left[\frac{Z_j A_{ij}^2 \ln A_{ij}}{\left(x_j + x_i A_{ij}\right)^2} + \frac{Z_i A_{ji}^2 \ln A_{ji}}{\left(x_i + x_j A_{ji}\right)^2}\right] \quad \ldots (4)$$

Eq. (4) can be used to calculate excess Gibbs free energy for a multicomponent mixture as (Tao, 2000):

$$\Delta G^{XS} = RT\left\{\sum_{i=1}^{N} x_i \ln \frac{V_{mi}}{\sum_{j=1}^{N} x_j V_{mj} A_{ji}} - \frac{1}{2}\sum_{i=1}^{N} Z_i x_i \left(\frac{\sum_{j=1}^{N} x_j A_{ji} \ln A_{ji}}{\sum_{k=1}^{N} x_k A_{ki}} \right)\right\} \quad \text{... (5)}$$

And the expression for the activity coefficient for the ith component, i.e., γ_i , is given by (Tao, 2000):

$$\ln \gamma_i = 1 + \ln \frac{V_{mi}}{\sum_{j=1}^{N} x_j V_{mj} A_{ji}} - \sum_{k=1}^{N} \frac{x_k V_{mi} A_{ik}}{\sum_{j=1}^{N} x_j V_{mj} A_{jk}} - \frac{1}{2}\left(\frac{Z_i \sum_{j=1}^{N} x_j A_{ji} \ln A_{ji}}{\sum_{l=1}^{N} x_l A_{li}} + \sum_{j=1}^{N} \frac{Z_j x_j A_{ij}}{\sum_{l=1}^{N} x_l A_{lj}} \times \left(\ln A_{ij} - \frac{\sum_{t=1}^{N} x_t A_{tj} \ln A_{tj}}{\sum_{l=1}^{N} x_l A_{lj}} \right) \right) \quad \text{... (6)}$$

where N represents the number of components in an alloy system.

Equation (7) is used in this study to obtain the value of Z_i (Tao, 2005):

$$Z_i = \frac{4\sqrt{2\pi}}{3}\left(\frac{r_{mi}^3 - r_{oi}^3}{r_{mi} - r_{oi}} \right) \rho_i r_{mi} \exp\left(\frac{\Delta H_{mi}(T_{mi} - T)}{Z_c R T T_{mi}} \right) \quad \text{... (7)}$$

where component i's melting point is denoted by T_{mi}; its melting enthalpy by ΔH_{mi}; its first peak value of radial distance by r_{mi}; and its close-packed coordination is by Z_c, and its value equals 12. $\tilde{n}_i$ represents the molecular number density and is given by, $\tilde{n}_i = \frac{N_i}{V_{mi}}$, where $N_i = 0.6022$ is the molecular number.

Table 1. Some input parameters (Iida & Guthrie, 1993).

i	ΔH_{mi} [KJ/mol]	r_{oi} [x10^{-8}cm]	r_{mi} [x10^{-8}cm]	V_{mi} [cm^3/mol]
Sn	7.07	2.68	3.14	17.00[1+0.87x10^{-4}(T-505)]
Sb	19.87	2.58	3.26	18.80[1+1.3x10^{-4}(T-904)]
Bi	11.30	2.78	3.34	20.80[1+1.17x10^{-4}(T-544)]

Equations (3) and (4), respectively, are used to derive the infinite dilution activity coefficients γ_i^{∞} and γ_j^{∞} as x_i and x_j approach zero, respectively (Tao, 2000):

$$\ln \gamma_i^{\infty} = 1 - \ln\left(\frac{V_{mj} A_{ji}}{V_{mi}} \right) - \frac{V_{mi} A_{ij}}{V_{mj}} - \frac{1}{2}\left(Z_i \ln A_{ji} + Z_j A_{ij} \ln A_{ij} \right) \quad \text{... (8)}$$

and

$$\ln \gamma_j^{\infty} = 1 - \ln\left(\frac{V_{mi} A_{ij}}{V_{mj}} \right) - \frac{V_{mj} A_{ji}}{V_{mi}} - \frac{1}{2}\left(Z_j \ln A_{ij} + Z_i A_{ji} \ln A_{ji} \right) \quad \text{... (9)}$$

The Newton-Raphson method is used to solve equations (8) and (9) to determine the values for A_{ji} and A_{ij}. The results of this computation serve as starting points for the

computation of component activity in liquid binary alloys using equations (3) and (4). Once the suitable A_{ji} and A_{ij} values are determined at a certain temperature, their equivalent values at subsequent temperatures can likewise be calculated (Tao, 2000). Now, the activity coefficient (γ_1) of the component metal 1 of the system can be gained from equation (5), treating the Sn-Sb-Bi ternary liquid alloy as the 1-2-3 system (Tao, 2000):

$$\ln\gamma_1 = 1+\ln\left(\frac{V_{m1}}{x_1V_{m1}+x_2V_{m2}A_{21}+x_3V_{m3}A_{31}}\right)-\frac{x_1V_{m1}}{x_1V_{m1}+x_2V_{m2}A_{21}+x_3V_{m3}A_{31}}-\frac{x_2V_{m1}A_{12}}{x_1V_{m1}A_{12}+x_2V_{m2}+x_3V_{m3}A_{32}}-\frac{x_3V_{m1}A_{13}}{x_1V_{m1}A_{13}+x_2V_{m2}A_{23}+x_3V_{m3}}$$

$$-\frac{1}{2}\left(\frac{Z_1\left(x_2A_{21}+x_3A_{31}\right)\left(x_2A_{21}\ln A_{21}+x_3A_{31}\ln A_{31}\right)}{\left(x_1+x_2A_{21}+x_3A_{31}\right)^2}+\frac{Z_2x_2A_{12}\left[\left(x_2+x_3A_{32}\right)\ln A_{12}-x_3A_{32}\ln A_{32}\right]}{\left(x_1A_{12}+x_2+x_3A_{32}\right)^2}+\frac{Z_3x_3A_{13}\left[\left(x_2A_{23}+x_3\right)\ln A_{13}-x_2A_{23}\ln A_{23}\right]}{\left(x_1A_{13}+x_2A_{23}+x_3\right)^2}\right) \quad \text{... (10)}$$

3. Results and Discussions

The expected values of the component's activities of liquid binary alloys Sb-Sn at 905 K, Bi-Sn at 600 K, and Bi-Sb at 1200 K were found by substituting the values of Z_i, Z_i, A_{ji}, and A_{ij} from Table 2 into Eqs. (3) and (4). Furthermore, the expected values of ΔG^{XS} for those binary liquid alloys were also computed from Eq. (1). The computed values of both components' activities and ΔG^{XS} for the binary liquid alloys have been reported in Tables 3, 4, and 5, respectively, by Hultgren et al. (Hultgren et al., 1973).

Table 2. Values Z_i, Z_j, A_{ji}, and A_{ij} for the binary alloys i-j at necessary temperatures.

i-j	T [K]	Z_i	Z_j	A_{ji}	A_{ij}
Sb-Sn	905	8.9614	8.5932	0.4743	1.7330
Bi-Sn	600	8.8699	9.1774	0.7661	1.1800
Bi-Sb	1200	7.5448	8.1760	1.8944	0.3318
Sb-Sn	900	8.9782	8.6005	0.4723	1.7383
Bi-Sn	900	8.0484	8.6005	0.8372	1.1166
Bi-Sb	900	8.0484	8.9782	2.3440	0.2297

Table 3. Theoretical and experimental (Hultgren et al., 1973) activities of components Sb and Sn along with ΔG^{XS} in the Sb-Sn system at 905 K.

X_{Sb}	X_{Sn}	a_{Sb} Th.	a_{Sb} Exp.*	a_{Sn} Th.	a_{Sn} Exp.*	ΔG^{XS} Th. [Cal/mol]	ΔG^{XS} Exp.* [Cal/mol]
0.000	1.000	0.000	0.000	1.000	1.000	0.0	0.0
0.100	0.900	0.048	0.049	0.895	0.892	-137.9	-144
0.200	0.800	0.11	0.113	0.778	0.772	-254.9	-256
0.300	0.700	0.190	0.194	0.649	0.646	-340.7	-336
0.400	0.600	0.288	0.290	0.519	0.520	-391.4	-384
0.500	0.500	0.401	0.400	0.395	0.400	-406.3	-400
0.600	0.400	0.525	0.520	0.285	0.290	-386.4	-384
0.700	0.300	0.651	0.646	0.190	0.194	-333.7	-336
0.800	0.200	0.776	0.772	0.112	0.113	-250.1	-256
0.900	0.100	0.893	0.892	0.049	0.049	-138.2	-144
1.000	0.000	1.000	1.000	0.000	0.000	0.0	0.0

It is noteworthy that Sb and Sn's activities in the Sb-Sn system at 905 K exhibit a notable agreement between predicted and experimental data, with minor discrepancies. The highest discrepancies noted are 2.65% for antimony (Sb) at X_{Sb} = 0.2 and 2.06% for tin (Sn) at X_{Sb} = 0.7, respectively.

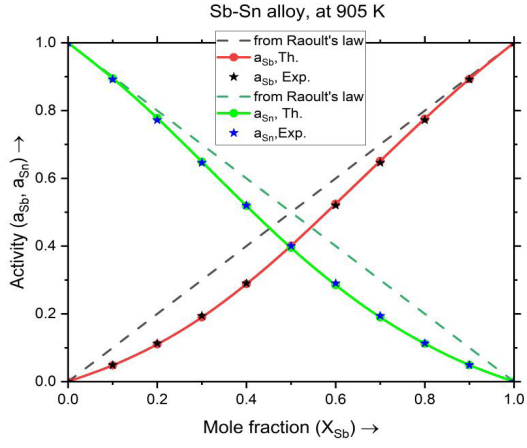

Figure 1. Theoretical and experimental (Hultgren et al., 1973) Sb and Sn's activities vs. X_{Sb} in the Sb-Sn system at 905 K.

Based on the information presented in Figure 1, it is obvious that there is a striking match between the predicted and observed activity data for antimony (Sb) and tin (Sn). The observed vapour pressures of each component inside the Sb-Sn mixture are lower at a temperature of 905 K than would be anticipated in a perfect mixture, according to the observed negative departure from Raoult's law. This means that the component has a stronger attraction to the other components in the mixture than is expected from ideal behavior.

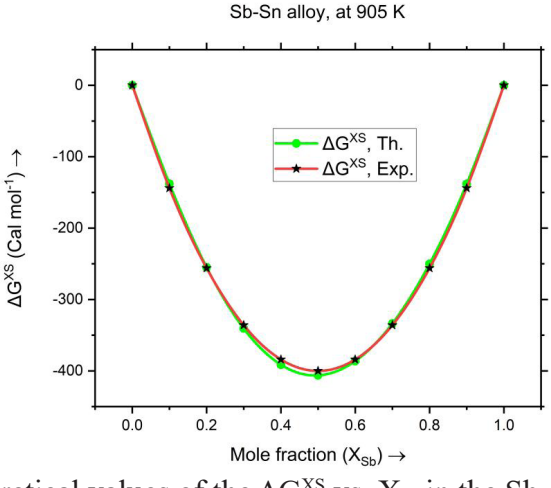

Figure 2. Theoretical values of the ΔG^{XS} vs. X_{Sb} in the Sb-Sn system at 905 K compared with the experimental results of Hultgren et al. (Hultgren et al., 1973).

The plot in Figure 2 illustrates the relationship between ΔG^{XS} and X_{Sb} for the Sb-Sn liquid system at 905 K. Although there are a few minor inconsistencies, the results show a significant agreement between theoretical predictions and practical observations, with the highest variation (4.23%) happening at $X_{Sb} = 0.1$. ΔG^{XS} continuously exhibits negative values over the full concentration range, peaking at -406.3 Cal/mol (theoretical) and -400 Cal/mol (experimental) when $X_{Sb} = 0.5$. These negative numbers denote a reduction in the mixture's volume relative to a perfect mixture after mixing.

Table 4. Theoretical and experimental (Hultgren et al., 1973) activities of components Bi and Sn along with ΔG^{XS} in the Bi-Sn system at 600 K.

X_{Bi}	X_{Sn}	a_{Bi} Th.	a_{Bi} Exp.*	a_{Sn} Th.	a_{Sn} Exp.*	ΔG^{XS} Th. [Cal/mol]	ΔG^{XS} Exp.* [Cal/mol]
0.000	1.000	0.000	0.000	1.000	1.000	0.0	0.0
0.100	0.900	0.124	0.124	0.904	0.904	30.9	31.0
0.200	0.800	0.231	0.232	0.813	0.813	51.1	51.0
0.300	0.700	0.330	0.331	0.724	0.723	62.5	63.0
0.400	0.600	0.424	0.426	0.632	0.632	66.5	67.0
0.500	0.500	0.517	0.519	0.538	0.537	64.6	66.0
0.600	0.400	0.611	0.613	0.439	0.439	57.8	59.0
0.700	0.300	0.706	0.706	0.335	0.337	47.1	49.0
0.800	0.200	0.802	0.802	0.227	0.229	33.5	34.0
0.900	0.100	0.900	0.900	0.115	0.116	17.5	18.0
1.000	0.000	1.000	1.000	0.000	0.000	0.0	0.0

It is noteworthy that Bi and Sn's activities in the Bi-Sn system at 600 K exhibit a notable concurrence between predicted and experimental data, with minor discrepancies. The highest discrepancies noted are 0.46% for bismuth (Bi) at a concentration of $X_{Bi} = 0.4$ and 0.87% for tin (Sn) at $X_{Bi} = 0.8$, respectively.

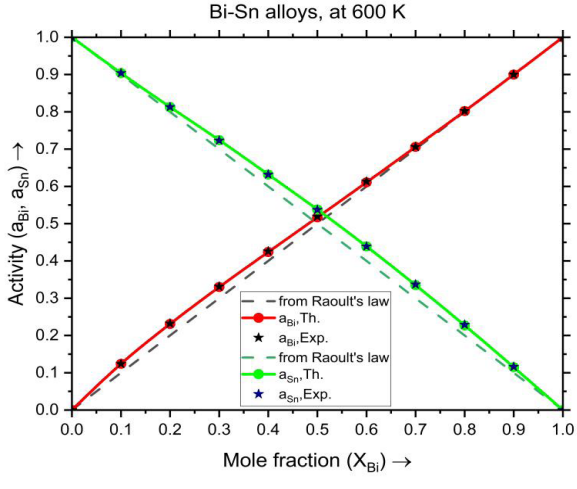

Figure 3. Theoretical and experimental (Hultgren et al., 1973) Bi and Sn's activities vs. X_{Bi} in the Bi-Sn system at 600 K.

Based on the information presented in Figure 3, it is obvious that there is a striking match between the predicted and experimental data of activity for bismuth (Bi) and tin (Sn). The observed vapour pressures of each component inside the Bi-Sn mixture are higher at a temperature of 600 K than would be anticipated in a perfect mixture, according to the observed positive departure from Raoult's law. This means that the component has a weaker attraction to the other components in the mixture than what is expected from ideal behavior.

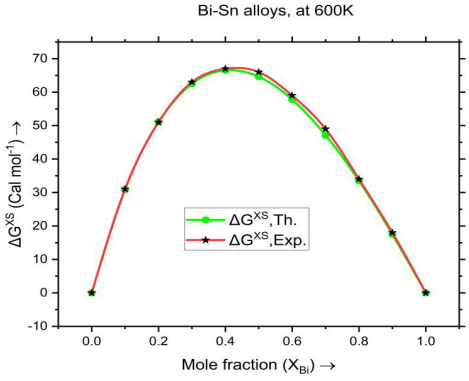

Figure 4. Theoretical values of the ΔG^{XS} vs. X_{Bi} in the Bi-Sn system at 600 K compared with the experimental results of Hultgren et al. (Hultgren et al., 1973).

The plot in Figure 4 illustrates the relationship between ΔG^{XS} and X_{Bi} for the Bi-Sn liquid system at 600 K. Although there are a few minor inconsistencies, the results show a significant agreement between theoretical predictions and practical observations, with the highest variation (3.87%) happening at $X_{Bi} = 0.7$. ΔG^{XS} continuously exhibits positive values over the full concentration range, peaking at 66.5 Cal/mol (theoretical) and 67 Cal/mol (experimental) when $X_{Bi} = 0.4$. These positive numbers denote an expansion in the mixture's volume relative to a perfect mixture after mixing.

Table 5. Theoretical and experimental (Hultgren et al., 1973) activities of components Bi and Sb along with ΔG^{XS} in the Bi-Sb liquid system at 1200 K.

X_{Bi}	X_{Sb}	a_{Bi} Th.	a_{Bi} Exp.*	a_{Sb} Th.	a_{Sb} Exp.*	ΔG^{XS} Th. [Cal/mol]	ΔG^{XS} Exp.* [Cal/mol]
0.000	1.000	0.000	0.000	1.000	1.000	0.0	0.0
0.100	0.900	0.052	0.050	0.892	0.895	-171.5	-176.0
0.200	0.800	0.120	0.112	0.773	0.780	-304.2	-323.0
0.300	0.700	0.208	0.187	0.646	0.659	-394.4	-438.0
0.400	0.600	0.315	0.278	0.516	0.533	-439	-515.0
0.500	0.500	0.441	0.397	0.392	0.398	-435.4	-548.0
0.600	0.400	0.580	0.571	0.281	0.255	-383.1	-501.0
0.700	0.300	0.718	0.749	0.189	0.154	-286.1	-363.0
0.800	0.200	0.837	0.865	0.119	0.101	-158.3	-177.0
0.900	0.100	0.924	0.929	0.067	0.067	-34.8	-28.0
1.000	0.000	1.000	1.000	0.000	0.000	0.0	0.0

It is noteworthy that Bi and Sb's activities in the Bi-Sb system at 1200 K exhibit a notable agreement between predicted and experimental data, with minor discrepancies. The highest discrepancies noted are 13.30% for bismuth (Bi) at $X_{Bi} = 0.4$ and 22.72% for antimony (Sb) at $X_{Bi} = 0.7$, respectively.

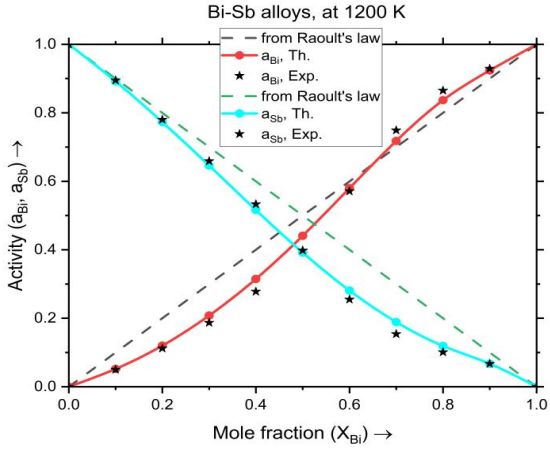

Figure 5. Theoretical and experimental (Hultgren et al., 1973) Bi and Sb's activities vs. X_{Bi} in the Bi-Sb system at 1200 K.

According to the data depicted in Figure 5, it becomes apparent that the anticipated and observed activity values for both bismuth (Bi) and antimony (Sb) within the Bi-Sb system at 1200 K exhibit a remarkable degree of similarity. Notably, the deviation in activity trends for Sb, in contrast to Raoult's line, displays a negative slope, while for Bi, it demonstrates a negative trend at lower X_{Bi} values and transitions to a positive trend at higher X_{Bi} values.

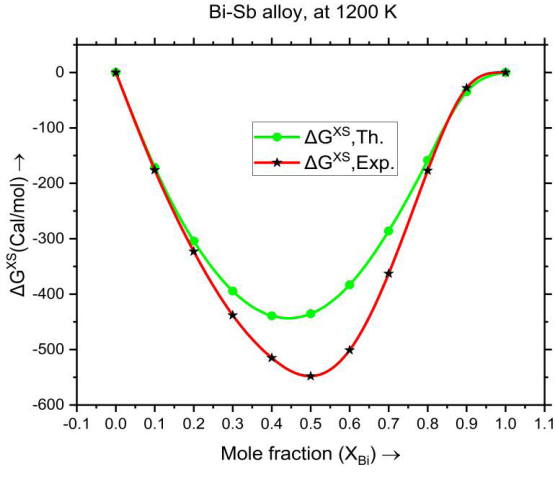

Figure 6. Theoretical values of the ΔG^{XS} vs. X_{Bi} in the Bi-Sb system at 1200 K compared with the experimental results of Hultgren et al. (Hultgren et al., 1973).

The plot in Figure 6 illustrates the relationship between ΔG^{XS} and X_{Bi} for the Bi-Sb liquid system at 1200 K. Although there are a few minor inconsistencies, the results show a significant concurrency between theoretical predictions and practical observations, with the highest variation (24.28%) happening at $X_{Bi} = 0.9$. ΔG^{XS} continuously exhibits negative values over the full concentration range, peaking at -439 Cal/mol (theoretical) and -548 Cal/mol (experimental) when $X_{Bi} = 0.5$. These negative numbers denote a reduction in the mixture's volume relative to a perfect mixture after mixing.

Table 6. Theoretical and experimental (Katayama et al., 2005) activities of Sn in the Sn-Sb-Bi liquid ternary system at 900 K.

Sb:Bi=1:3			$a_{Sn, Th.}$	$a_{Sn, Exp.*}$	$\lvert a_{Sn, Th.} - a_{Sn, Exp.*} \rvert$	Percentage Error (%)
X_{Sn}	X_{Sb}	X_{Bi}				
1.000	-------	-------	1.000	-------	-------	-------
0.800	0.050	0.150	0.820	0.802	0.018	2.24
0.700	0.075	0.225	0.731	0.713	0.018	2.52
0.600	0.100	0.300	0.638	0.594	0.044	7.40
0.500	0.125	0.375	0.538	0.488	0.050	10.24
0.400	0.150	0.450	0.433	0.380	0.053	13.94
0.300	0.175	0.525	0.325	0.278	0.047	16.90
0.200	0.200	0.600	0.216	0.177	0.039	22.03
0.100	0.225	0.675	0.106	0.089	0.017	19.10
0.000	-------	-------	0.000	-------	-------	-------
Sb:Bi=1:1						
1.000	-------	-------	1.000	-------	-------	-------
0.800	0.100	0. 100	0.817	0.794	0.023	2.89
0.700	0.150	0.150	0.723	0.680	0.043	6.32
0.600	0.200	0.200	0.622	0.566	0.056	9.89
0.500	0.250	0.250	0.516	0.468	0.048	10.25
0.400	0.300	0.300	0.408	0.350	0.058	16.57
0.300	0.350	0.350	0.300	0.217	0.083	38.24
0.200	0.400	0.400	0.195	0.150	0.045	30.00
0.100	0.450	0.450	0.094	0.068	0.026	38.23
0.000	-------	-------	0.000	-------	-------	--------
Sb:Bi=3:1						
1.000	-------	-------	1.000	-------	-------	------
0.800	0.150	0.050	0.802	0.790	0.012	1.51
0.700	0.225	0.075	0.693	0.662	0.031	4.68
0.600	0.300	0.100	0.577	0.541	0.036	6.65
0.500	0.375	0.125	0.461	0.421	0.040	9.50
0.400	0.450	0.150	0.349	0.354	0.005	1.41
0.300	0.525	0.175	0.245	0.211	0.034	16.11
0.200	0.600	0.200	0.152	------	------	-------
0.100	0.675	0.225	0.070	0.063	0.007	11.11
0.000	-------	-------	0.000	-------	-------	-------

$S_{Sn}^{*} = \pm 0.0406\%$, $S_{Sn} = \pm 12.94\%$

Table 6 presents the estimated Sn activities in Sn-Sb-Bi liquid ternary alloys at 900 K using Eq. (10), and the results are contrasted with the reference's experimental data (Katayama et al., 2005). With the exception of a few variations, the agreement between our computed activities and the experimentally measured values is satisfactory across all three sections of Sb:Bi = 1:3, 1:1, and 3:1. Here, the concentrations of the first component, i.e., Sn, vary between 0 and 1.

To accurately quantify the magnitude of the deviation between experimental values and estimated data, the average standard deviation S_i^* and average relative error S_i have been calculated from Table 6.

The average standard deviation can be given by the equation

$$S_i^* = \pm[\frac{1}{n}\sum_{i=1}^{n}(a_i, \text{Th.} - a_i, \text{Exp.}*)^2]^{\frac{1}{2}} \quad \text{... (11)}$$

The average relative error can be given by the equation

$$S_i = \pm\frac{100}{n}\sum_{i=1}^{n}\left|\frac{a_i,\text{Th.} - a_i,\text{Exp.}*}{a_i,\text{Exp.}*}\right| \quad \text{... (12)}$$

In the current study, the number of experimental data points (n) has been taken as 23. So, the calculated values of the standard deviation and average relative error are found to be $\pm 0.0406\%$ and $\pm 12.94\%$, respectively.

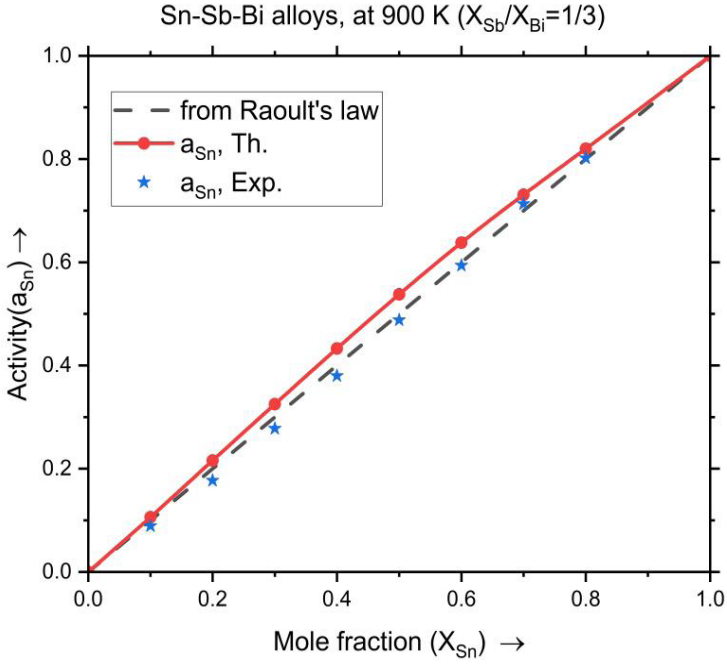

Figure 7. Activities of Sn vs. X_{Sn} in the section Sb:Bi = 1:3 of the Sn-Sb-Bi alloy at 900 K, predicted and experimental (Katayama et al., 2005).

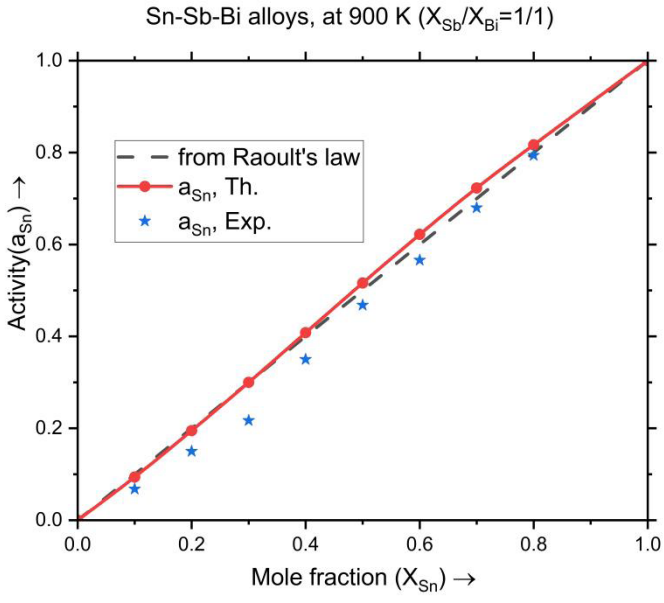

Figure 8. Activities of Sn vs. X_{Sn} in the section Sb:Bi = 1:1 of the Sn-Sb-Bi alloy at 900 K, predicted and experimental (Katayama et al., 2005).

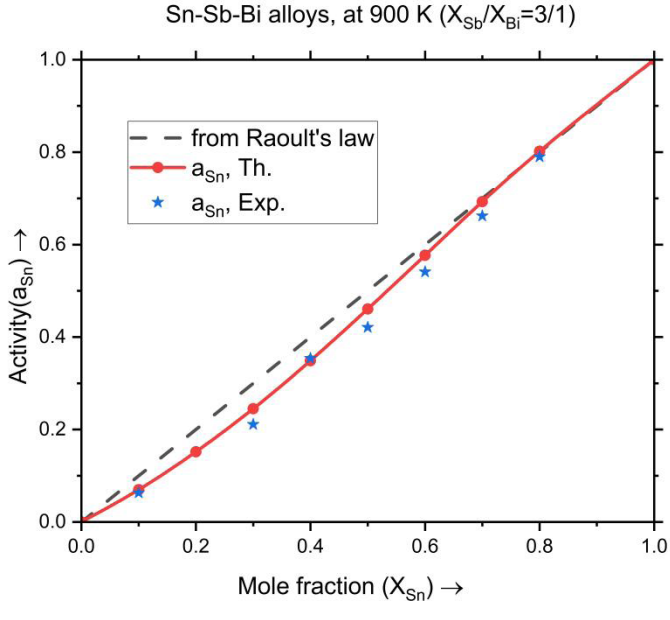

Figure 9. Activities of Sn vs. X_{Sn} in the section Sb:Bi = 3:1 of the Sn-Sb-Bi alloy at 900 K, predicted and experimental (Katayama et al., 2005).

Figure 7 shows that, in the concentration range of $0.3 < X_{Sn} < 0.7$, the predicted activities of tin (Sn) in the Sn-Sb-Bi alloys exhibit a modest positive divergence from the ideal Raoult's line at 900 K. Furthermore, these theoretical activities deviate from the experimental values, with the highest variation of 22.03% at a concentration of X_{Sn} = 0.2, especially for the Sb: Bi cross-section of 1:3. The positive departure from Raoult's law indicates that the observed vapour pressures of the component Sn inside the Sn-Sb-Bi mixture are higher at a temperature of 900 K than would be anticipated in a perfect mixture. This means that the component has a weaker attraction to the other components in the mixture than is expected from ideal behavior.

In a comparable fashion, Figure 8 illustrates that the theoretical behavior of Sn in the identical alloy displays a slight positive departure from the ideal Raoult's line when the concentration falls within the range of $0.4 < X_{Sn} < 0.8$ and a very small negative departure in the range of $0.1 < X_{Sn} < 0.2$. This shows that the Sn activity curve is very close to the ideal raoult's line when Sb:Bi=1:1. These theoretical deviations from the experimental data reach their highest point, with a maximum error of 38.24%, occurring at concentration X_{Sn} = 0.3 for the Sb:Bi ratio of 1:1.

In contrast, Figure 9 shows that when the concentration is between $0.1 < X_{Sn} < 0.6$, the theoretical behaviors of Sn in the Sn-Sb-Bi system show a slight negative departure from the ideal Raoult's line. At X_{Sn} = 0.3, where the maximum errors of 16.11% occur, these theoretical departures from the experimental results are at their greatest significance. They are especially obvious when the Sb:Bi ratio is 3:1. This negative deviation implies that the partial vapour pressures of Sn in the Sn-Sb-Bi system, especially in the case of a 3:1 Sb:Bi mixture, are lower than what would be anticipated in an ideal mixture situation at 900 K.

Sn-Sb-Bi solder alloys are significant in the context of lead-free soldering due to their environmental friendliness, compliance with regulations, lower melting temperature, reliability, and suitability for various electronic soldering applications, especially those involving fine-pitch components.

4. Conclusion

Our theoretical analysis strongly indicates that the MIVM serves as an appropriate framework for characterizing the thermodynamic properties, including component activity and ΔG^{XS}, in liquid binary alloys that are free of lead. Moreover, our analysis indicates that this model can be extended to comprehend the thermodynamics of lead-free ternary liquid alloys as well. The positive divergence in the activities of component metals within Bi-Sn systems and the negative deviation in the activities of constituent metals within Sb-Sn systems from the ideal mixing behavior are both satisfactorily explained by the theoretical explanation. Additionally, the model offers a convincing justification for the coexistence of both negative and positive deviations in the behavior of the Bi component, as well as the negative deviation shown in the case of the Sb

component within the context of the Bi-Sb system. Concerning the Sn-Sb-Bi system, the investigation reveals that the activity of Sn displays positive deviations for the cross-sections of Sb:Bi = 1:3 and both small negative and positive deviations for Sb:Bi=1:1, whereas a negative deviation is observed for the Sb:Bi = 3:1 cross-section. In all cases, these deviations diverge from the behavior expected in ideal mixing scenarios. These findings are successfully accounted for by the proposed theoretical model. Notably, the study reveals that the deviations in Sn activities within ternary Sn-Sb-Bi alloys change from positive to negative as the Sb content increases along the three cross-sections, namely Sb:Bi = 1:3, 1:1, and 3:1.

The study of the thermodynamic properties of Sn-Sb-Bi liquid alloys has broad implications for various industries. It can lead to the development of new solder materials, improved manufacturing processes, enhanced environmental sustainability, better performance in electronic devices, and other critical technologies.

References

Abtew, M., & Selvaduray, G. (2000). Lead-free solders in microelectronics. *Materials Science and Engineering R: Reports*, *27*(5–6), 95–141. https://doi.org/10.1016/S0927-796X(00)00010-3

Adedipe, A. M., Odusote, Y. A., Ndukwe, I. C., & Madu, C. A. (2019). Energetics of compound formation in liquid Bi-Sb , Bi-Sn , and Sb-Sn binary alloys. *Phys. J.*, *3*, 37–48.

Almeida, C. M. V. B., Madureira, M. A., Bonilla, S. H., & Giannetti, B. F. (2013). Assessing the replacement of lead in solders: Effects on resource use and human health. *Journal of Cleaner Production*, *47*, 457–464. https://doi.org/10.1016/j.jclepro.2012.08.002

Amore, S., Ricci, E., Lanata, T., & Novakovic, R. (2008). Surface tension and wetting behaviour of molten Cu-Sn alloys. *Journal of Alloys and Compounds*, *452*(1), 161–166. https://doi.org/10.1016/j.jallcom.2007.01.178

Anusionwu, B. C. (2006). Thermodynamic and surface properties of Sb-Sn and In-Sn liquid alloys. *Pramana - Journal of Physics*, *67*(2), 319–330. https://doi.org/10.1007/s12043-006-0076-z

Asryan, N.A., & Mikula, A. (2004). Thermodynamic properties of Bi-Sn melts. *Inorganic Materials*, *40*, 386–390.

Awe, O. E., & Oshakuade, O. M. (2014). Theoretical prediction of thermodynamic activities of all components in the Bi-Sb-Sn ternary lead-free solder system and Pb-Bi-Sb-Sn quaternary system. *Thermochimica Acta*, *589*, 47–55. https://doi.org/10.1016/j.tca.2014.05.009

Hindler, M., Knott, S., & Mikula, A. (2010). Thermodynamic properties of liquid Ag-Au-Sn alloys. *Journal of Electronic Materials*, *39*(10), 2310–2315. https://doi.org/10.1007/s11664-010-1292-3

Hultgren, R. R., Desai, P. D., Hawkins, D. T., Gleiser, M., Kelley, K. K., & Wagman, D. D. (1973). *Selected values of the thermodynamic properties of binary alloys*. National Standard Reference Data System, New york.

Iida, T., & Guthrie, R. I. L. (1993). *The Physical Properties of Liquid Metals*. Clarendon Press, Oxford.

Katayama, I., Zivkovic, D., Manasijevic, D., Tanaka, T., Zivkovic, Z., & Yamashita, H. (2005).

Thermodynamic Properties of Liquid Sn-Bi-Sb Alloys. *Netsu Sokutei*, *32*(1), 40–44. https://doi.org/https://doi.org/10.11311/jscta1974.32.40

Knott, S., & Mikula, A. (2002). Thermodynamic properties of liquid Al-Sn-Zn alloys: A possible new lead-free solder material. *Materials Transactions*, *43*(8), 1868–1872. https://doi.org/10.2320/matertrans.43.1868

Lee, J., Shimoda, W., & Tanaka, T. (2004). Surface Tension and its Temperature Coefficient of Liquid Sn-X (X = Ag , Cu) Alloys. *Materials Transactions*, *45*(9), 2864–2870.

Liang, L. M., Ding, G. H., Wang, Y. X., & Liu, Y. (2021). Thermodynamic properties of liquid Zn-Cd alloys investigated by the molecular interaction volume model. *Physics and Chemistry of Liquids*, *59*(5), 706–715. https://doi.org/10.1080/00319104.2020.1808655

Moelans, N., Hari Kumar, K. C., & Wollants, P. (2003). Thermodynamic optimization of the lead-free solder system Bi-In-Sn-Zn. *Journal of Alloys and Compounds*, *360*(1–2), 98–106. https://doi.org/10.1016/S0925-8388(03)00325-6

Odusote, Y. A., Popoola, A. I., & Oluyamo, S. S. (2016). Bulk and surface properties of demixing liquid Al–Sn and Sn–Tl alloys. *Applied Physics A: Materials Science and Processing*, *122*(2), 1–9. https://doi.org/10.1007/s00339-015-9591-4

Sah, S. K., Jha, I. S., & Koirala, I. (2022). Computational Study of the Thermodynamic Properties of Some Lead-free Solder Alloys. *BMC Journal of Scientific Research*, *5*(1), 69–79. https://doi.org/DOI: https://doi.org/10.3126/bmcjsr.v5i1.50676

Sah, S. K., Jha, I. S., & Koirala, I. (2023). Theoretical Examination of Some Thermodynamic Properties in In - Bi - Sn Liquid Alloy and its Sub - binary Systems. *Journal of Electronic Materials*, *0123456789*. https://doi.org/10.1007/s11664-023-10571-y

Sah, S. K., & Koirala, I. (2023). Computational assessment of Sn activities and integral excess free energy change for mixing in the Sn-Au-Cu ternary liquid alloys using the molecular interaction volume model. *Journal of Physics Communications*, *m*. https://doi.org/https://doi.org/10.1088/2399-6528/ad035a

Sah, S. K., Koirala, I., & Jha, I. S. (2023). Theoretical investigation of the thermodynamic activities of Zn-In-Sn lead-free solder alloys and the concerned binary alloys. *Materials Today: Proceedings*, *xxxx*. https://doi.org/10.1016/j.matpr.2023.03.078

Suganuma, K. (2001). Advances in lead-free electronics soldering. *Current Opinion in Solid State and Materials Science*, *5*(1), 55–64. https://doi.org/10.1016/S1359-0286(00)00036-X

Tao, D. P. (2000). A new model of thermodynamics of liquid mixtures and its application to liquid alloys. *Thermochimica Acta*, *363*(1–2), 105–113. https://doi.org/10.1016/S0040-6031(00)00603-1

Tao, D. P. (2005). Prediction of the coordination numbers of liquid metals. *Metallurgical and Materials Transactions A*, *36*(12), 3495–3497. https://doi.org/10.1007/s11661-005-0023-5

Tao, D. P. (2008). Prediction of activities of all components in the lead-free solder systems Bi-In-Sn and Bi-In-Sn-Zn. *Journal of Alloys and Compounds*, *457*(1–2), 124–130. https://doi.org/10.1016/j.jallcom.2007.02.123

Tao, D. P., Yang, B., & Li, D. F. (2002). Prediction of the thermodynamic properties of quinary liquid alloys by modified coordination equation. *Fluid Phase Equilibria*, *193*, 167–177.